Mechanics of Advanced Composite Structures 5 (2018) 41–48

Semnan University

Mechanics of Advanced Composite Structures

journal homepage: http://MACS.journals.semnan.ac.ir

Experimental Study on Amine-Functionalized Carbon Nanotubes' Effect on the Thermomechanical Properties of CNT/Epoxy Nanocomposites

S.M. Hosseini Farrash[a], J. Rezaeepazhand [b*], M. Shariati[a]

[a]*Nanomechanics Lab., Department of Mechanical Engineering, Ferdowsi University of Mashhad, Mashhad, 9177948974, Iran*
[b]*Smart and Composite Structures Lab., Department of Mechanical Engineering, Ferdowsi University of Mashhad, Mashhad, 9177948974, Iran*

PAPER INFO

Paper history:
Received 2017-04-08
Revised 2017-06-18
Accepted 2017-07-01

Keywords:
Functionalization
Carbon nanotubes
Nanocomposites
Thermomechanical properties

ABSTRACT

This paper investigated the effect of the amine-functionalized carbon nanotubes (CNTs) on the thermomechanical properties of CNT/epoxy nanocomposites. Mechanical stirring and ultra-sonication were utilized to uniformly disperse CNTs into the epoxy matrix. Non-functionalized and amine-functionalized CNTs with different weight percentages (wt. %) were mixed into the epoxy resin. Using standard tensile and dilatometry test specimens, this paper determined Young's modulus, ultimate strength, strain at break, coefficients of thermal expansion, glass transition temperature (T_g), and thermal strain at T_g of the specimens. Neat epoxy, non-functionalized CNT/epoxy (0.25 and 0.5 wt. % CNTs), and functionalized CNT/epoxy (0.25 and 0.5 wt. % functionalized CNTs) nanocomposites were studied. The results indicated that adding 0.25 wt. % functionalized CNTs into the epoxy resin had the greatest effect on Young's modulus and the nanocomposites' coefficient of thermal expansion. Moreover, adding CNTs into the epoxy resin decreased the ultimate strength, strain at break, and coefficient of thermal expansion of the specimens.

1. Introduction

Since the discovery of carbon nanotubes (CNTs) in 1991 by Iijima [1], CNTs' substantial properties have been reported by several researchers. CNTs with remarkable mechanical, thermal, and electrical properties have received intensive attention in recent years [2]. When CNTs are added into epoxy as nanofillers, a CNT/epoxy nanocomposite with enhanced thermomechanical properties is formed. To achieve the improved properties of nanocomposites, CNTs should be dispersed homogenously into the matrix material. When the weight percentage (wt. %) of CNTs increases in a nanocomposite, the van der Waals attractive forces between the nanotubes prevent the uniform dispersion of CNTs into the matrix material. Chemical functionalization of CNTs is a method used to achieve a good distribution of CNTs in the epoxy polymer. In this method, a chemical group, such as hydroxyl (–OH), carboxyl (–COOH), or amine (–NH2), is attached to the CNT and reacted with the epoxy or curing agent (or both) during the curing process. These functional groups also decrease the van der Waals forces between the CNTs and prevent the CNTs' agglomeration into the epoxy matrix. Bukowska et al. [3] synthesized and characterized functionalized Fe_3O_4 nanoparticles for various applications (such as drug delivery systems.) Ma et al. [4] manufactured CNT/epoxy composites and demonstrated that amine-functionalized CNTs

* Corresponding author. Telefax.: +98-51-38806055

E-mail address: jrezaeep@um.ac.ir

through covalent bonds resulted in improved flexural and thermo-mechanical properties compared with those without functionalization. Gojny et al. [5] produced nanocomposites consisting of double-walled CNTs and an epoxy matrix. They employed a shear mixing (calendar) technique to improve the dispersion of CNTs in the matrix. They used pure CNTs and functionalized CNTs with different wt. % to investigate the mechanical properties of the nanocomposites. Bal et al. [6] manufactured CNT/epoxy composites and investigated the flexural modulus and hardness of the specimens that had been subjected to different temperature conditions. They also examined the influence of the temperature on the mechanical properties of the nanocomposites. Sharma and Shukla [7] investigated the effect of the amine functionalization of CNTs on the mechanical properties of multiscale composites. They fabricated and tested CNT/carbon/epoxy standard specimens. Kazemi et al. [8] added calcium hydroxide nanoparticles and aminated multi-walled CNTs (MWCNTs) into a paraloid resin. They stated that the obtained nanocomposite can be used by monuments as a protective layer against acid rain and extreme heat. Ghorbanali et al. [9] investigated the effect of magnesium hydroxide and modified MWCNTs on the thermal stability of the cellulose acetate (CA). Moaseri et al. [10] carried out single fiber tensile testing and demonstrated that the functionalization of carbon fibers can improve the mechanical properties of composites remarkably. Shariati et al. [11] added silica nanoparticles into the epoxy resin; they studied the effect of silica wt. % and particle size on Young's modulus, yield strength, and energy absorption of thin-walled square columns. Shahrajabian et al. [12] studied the influence of electron beam irradiation on the thermal and mechanical properties of vinyl-ester/Tio2 nanocomposites. Parvaneh and Shariati [13] presented a new method for fabricating CNT/polymer nanocomposites. Mehdizadeh and Jahangiri [14] investigated the influence of adding carbon black (CB) into the epoxy resin on the wave absorbing of the CB/epoxy nanocomposite. Hejri et al. [15] homogenously dispersed TiO_2 nanoparticles into the vinyl alcohol and investigated the mechanical and thermal behavior of the nanocomposite films. Lu et al. [16] added functionalized MWCNTs into the natural rubber and investigated the mechanical, thermal, and electrical properties of the obtained nanocomposite.

Furthermore, the mechanical properties of nanocomposites have been studied theoretically by some researchers. Odegard et al. [17] developed constitutive models to determine the bulk mechanical properties of CNT/polymer nanocomposites. Seidel et al. [18] used micromechanics techniques to obtain the elastic properties of CNT-reinforced composites. They also compared their results with finite element simulations and experimental data. Han and Elliott [19] utilized molecular dynamic (MD) simulations to calculate the elastic modulus of CNT/polymer nanocomposites. They added single-walled CNTs that had different wt. % into the two different polymer matrices; this was done to study the nanocomposite's mechanical properties. Additionally, they compared their results with those from the rule of mixtures. Arash et al. [20] used MD simulations and presented a new method for estimating the elastic properties of the interfacial region of a CNT-reinforced poly methyl methacrylate (PMMA) composite under tension. Le and Huang [21] employed representative volume elements and extracted the effective elastic constants of CNT-dispersed nanocomposites. They used the extended rule of mixture to validate the proposed model. Rostmiyan et al. [22] conducted experiments and employed surface design methodology to enhance the flexural strength of an epoxy-based nanocomposite.

To the authors' best knowledge, little research exists on the thermomechanical properties of amine-functionalized CNT-reinforced epoxy composites. The fabrication of CNT/epoxy composite specimens were done with two different CNT weight percentages (0.25 wt. % and 0.5 wt. %) of non-functionalized and amine-functionalized CNTs to compare the effects of functionalization. Mechanical stirring and ultra-sonication were employed to uniformly disperse CNTs into the epoxy matrix. Utilizing the tensile and dilatometry tests, this study determined Young's modulus, ultimate strength, strain at break, coefficients of thermal expansion (CTE), glass transition temperature (T_g), and thermal strain at T_g of the specimens. Transmission electron microscopy (TEM) images of CNTs were taken to show the morphology of the CNTs. Furthermore, scanning electron microscopy (SEM) images of the tensile test specimens' fracture surfaces were prepared to illustrate the dispersion quality of CNTs into the matrix material.

2. Experiment

2.1 Materials

Epolam 2040 resin and Epolam 2047 hardener (Axson Technologies, France) were used in this study. MWCNTs and amine-functionalized MWCNTs (AFMWCNTs) with a purity $> 95\%$ were obtained from Carbon Structure Company. Fig. 1 shows the TEM images of MWCNTs. Fig. 2 illustrates the Fourier transform infrared (FTIR) spectroscopy of the AFMWCNTs. In the figure, the peak of 3448.38 cm^{-1} corresponds to the amine stretch vibrational mode.

2.2 Fabrication process

Tensile and dilatometry test specimens were fabricated according to ASTM D638 and ASTM E831 standards, respectively. Neat epoxy, epoxy reinforced with MWCNT (0.25 wt. % and 0.5 wt. % MWCNTs), and epoxy reinforced with AFMWCNT (0.25 wt. % and 0.5 wt. % AFMWCNTs) specimens were manufactured. Mechanical stirring and the ultra-sonication method were utilized to uniformly disperse CNTs into the epoxy resin. First, using a magnetic stirrer with a heater, CNTs were mechanically mixed into the epoxy resin for 15 min at 60°C. Then, an Elma ultrasonic bath (S40 H, 340 W, 37 KHz) was employed for 2 hours to completely disperse the CNTs into the epoxy resin. Next, the hardener was added into the CNT/epoxy mixture, and the obtained mixture was degassed in a desiccator chamber using a vacuum for 30 minutes (Fig. 3). The bubble-free CNT-epoxy mixture was molded and cured for 24 h at room temperature. Finally, the specimens were post-cured for 16 h at 70°C. Fig. 4 shows the manufactured neat epoxy and CNT/epoxy test specimens.

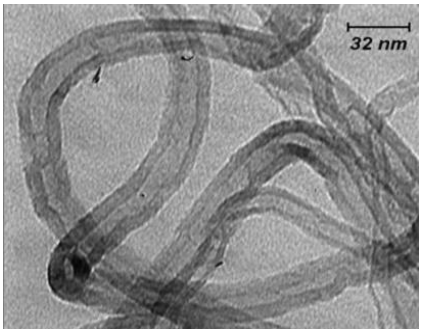

Figure 1. TEM image of MWCNTs

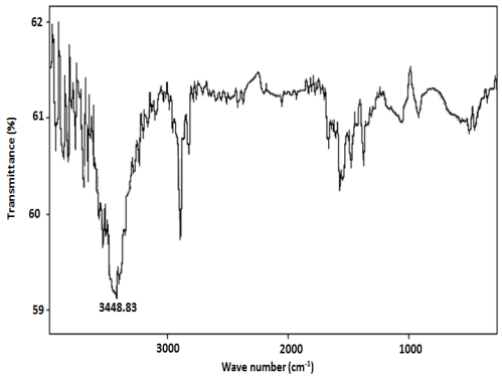

Figure 2. FTIR spectroscopy of the amine-functionalized multi-walled CNTs

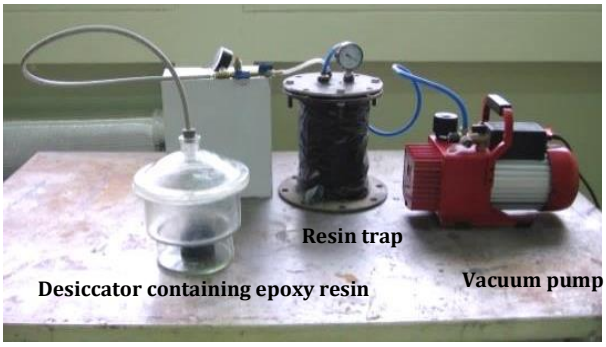

Figure 3. Degassing of the epoxy resin using a vacuum pump

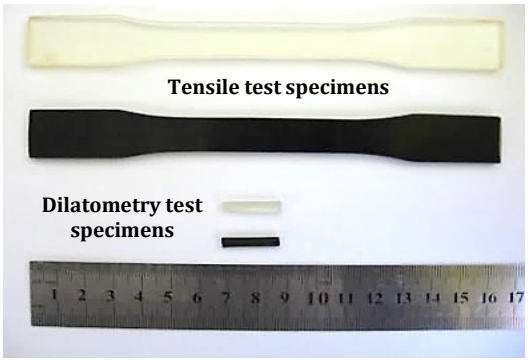

Figure 4. Tensile and dilatometry test specimens with and without MWCNTs

2.3 Test procedures

A Zwick Z250 materials testing machine was employed to perform the tensile tests. Young's modulus (E), the ultimate strength (S_{ut}), and the strain at break (ε_b) of the specimens were obtained from the stress-strain curves. Moreover, a horizontal dilatometer (LINSEIS 70/2171, Germany) was operated to determine the CTE (α), glass transition temperature (T_g), and thermal strain at the glass transition temperature (ε_{T_g}) of the specimens.

The dilatometer is illustrated in Fig. 5. The main advantage of the horizontal system is the uniform temperature distribution that was present all over the specimen. The specimen was located between the end of the sample holder and the probe rod, which was connected to the displacement sensor assembly outside the furnace. A typical dilatometric output curve is shown in Fig. 6. This graph displays sample length change (ΔL) versus sample temperature. The CTE of the specimen was calculated from the slope of the linear part of this curve as follows:

$$\alpha = \frac{1}{L_0}\frac{\Delta L}{\Delta T} \tag{1}$$

where L_0 is the initial length of the specimen and ΔT is the temperature increase that causes ΔL.

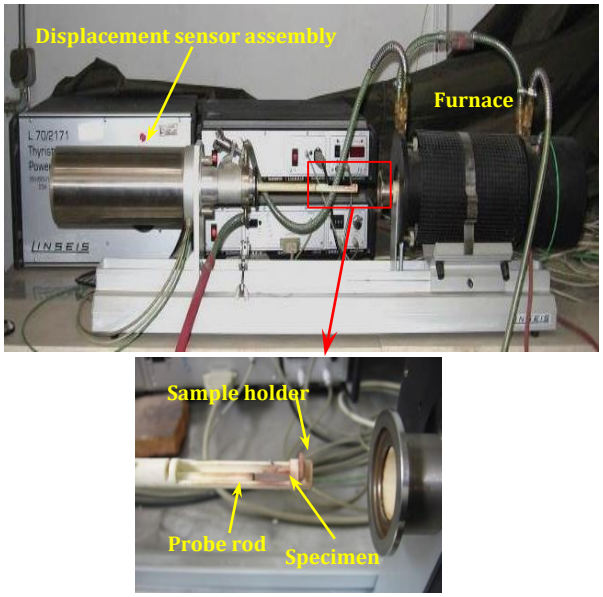

Figure 5. Horizontal dilatometer

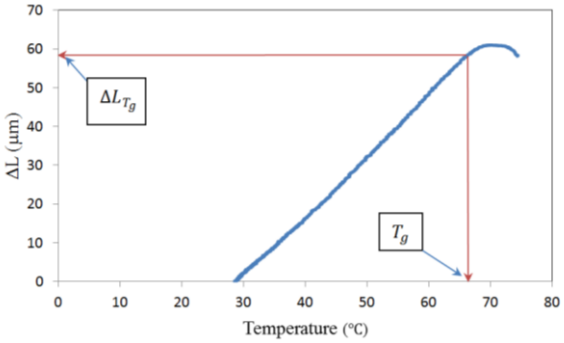

Figure 6. A typical dilatometric curve (change in length vs. temperature): α, T_g, and ΔL_{T_g} are extracted from this curve

The glass transition temperature (T_g) is one of the most important properties of polymers; it is the temperature at which the polymer transitions from a hard material to a soft and rubbery material. As can be seen in Fig. 6, a great change in the CTE amount of the sample specifies this parameter. ΔL_{T_g} is the length increase of the specimen at T_g. The thermal strain at the glass transition temperature is defined as:

$$\varepsilon_{T_g} = \frac{\Delta L_{T_g}}{L_0} \tag{2}$$

3. Results and Discussion

In this section, the effect of the MWCNTs and AFMWCNTs' dispersion into the epoxy resin on the thermomechanical properties of the epoxy resin is presented. In each case, five test specimens were tested, and the average values were reported. SEM images of the tensile specimens' fracture surface justified the results.

3.1 Thermomechanical properties

The results are summarized in Table 1. To facilitate the result statement, a code was specified for each specimen in this table, for example EP stands for epoxy. Based on Table 1, Young's modulus of the neat epoxy was 2.83 (GPa). Moreover, to compare the results, all thermomechanical properties of the specimens were normalized with respect to the same property of the neat epoxy specimen. The normalized properties are shown in figures 7–12.

Table 1. Young's modulus, ultimate strength, strain at break, and CTE of the fabricated specimens

Specimen	Code	$E\ (GPa)$	$S_{ut}\ (MPa)$	ε_b (%)	α (μ/°C)	T_g(°C)	ε_{T_g}(%)
Epoxy	EP	2.83	74.66	4.79	73.38	66.8	0.28
CNT/epoxy (0.25 wt. % of MWCNTs)	EP+0.25%CNTs	2.93	59.61	2.07	61.13	61.9	0.23
CNT/epoxy (0.5 wt. % of MWCNTs)	EP+0.5%CNTs	2.57	55.19	2.12	64.53	71.4	0.30
CNT/epoxy (0.25 wt. % of AFMWCNTs)	EP+0.25%AFCNTs	3.42	66.92	2.79	60.39	75.7	0.21
CNT/epoxy (0.5 wt. % of AFMWCNTs)	EP+0.5%AFCNTs	3.29	61.94	2.52	61.96	73.9	0.27

As Fig. 7 shows, adding 0.25 wt. % MWCNTs into the epoxy resin caused a 4% increase in this parameter's amounts. When the wt. % of the dispersed MWCNTs increased to 0.5 wt. %, the nanocomposite's Young's modulus decreased approximately 9% compared to that of the EP.

Moreover, adding 0.25 wt. % functionalized MWCNTs into the matrix material developed a 21 % increase in the amount of the epoxy's Young's modulus, which was 17% more than that of the EP+0.25%CNT nanocomposite. Additionally, when the wt. % of AFMWCNTs increased to 0.5%, the normalized Young's modulus of the nanocomposite reached 1.16, which was 5% less than that of the EP+0.25%FCNT nanocomposite. These results showed that CNT functionalization leads to a better dispersion of CNTs in the epoxy matrix; however, CNT agglomeration occurred when the CNT wt. % increased.

Figures 8 and 9 display the effect of adding MWCNTs and AFMWCNTs in the epoxy resin on the ultimate strength and the strain at break of the nanocomposites, respectively. Based on these figures, both of these parameters were reduced when MWCNTs or AFMWCNTs were added into the matrix material. The highest reduction in ultimate strength was related to the EP+0.5%CNT nanocomposite, which showed a 26% decrease in its ultimate strength compared to that of the neat epoxy. Moreover, the normalized strain at break of the EP+0.25%CNT nanocomposite was 0.43, which was the lowest value among all the examined specimens.

Fig. 10 represents the variations of the CTE of the epoxy due to MWCNTs and AFMWCNTs being added. As expected, because of the negative CTE of the carbon material, when MWCNTs or AFMWCNTs are distributed into the epoxy resin, the CTE of the nanocomposite decreases. The greatest reduction of the CTE was 17% with respect to that of the neat epoxy that was related to the EP+0.25%AFCNTs, which CNTs dispersed well into the matrix material.

Figures 11 and 12 illustrate the specimens' T_g and the thermal strain at T_g, respectively. As can be seen in Fig. 11, the maximum value of glass transition temperature is related to EP+0.25%AFCNTs sample. Moreover, based on Fig. 12, this specimen has the minimum value of a thermal strain at the glass transition temperature. Strong adhesion between AFMWCNTs and the polymer matrix increased T_g and led to the reduction of ε_{T_g} for this specimen.

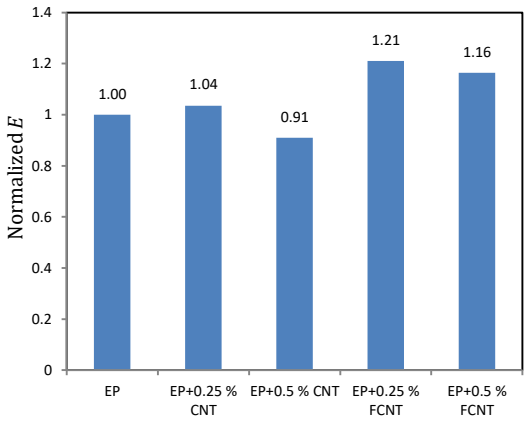

Figure 7. Normalized Young's modulus of the nanocomposites

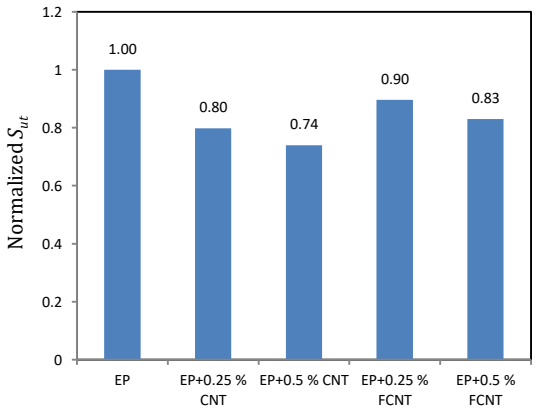

Figure 8. Normalized ultimate strength of the nanocomposites

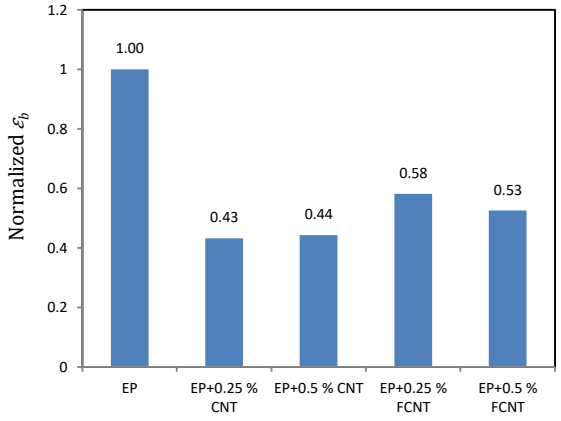

Figure 9. Normalized strain at break of the nanocomposites

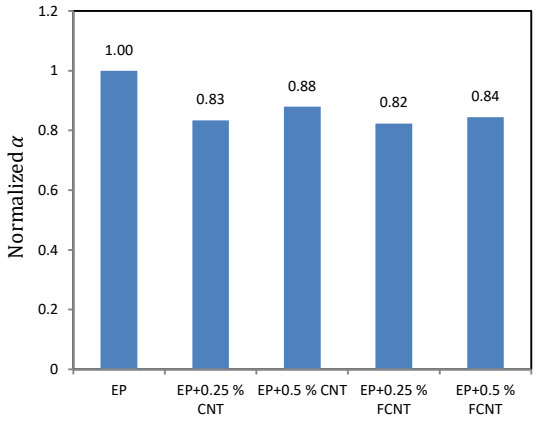

Figure 10. Normalized CTE of the nanocomposites

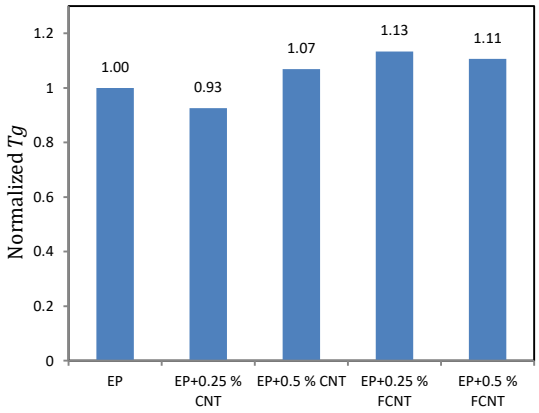

Figure 11. Normalized T_g of the nanocomposites

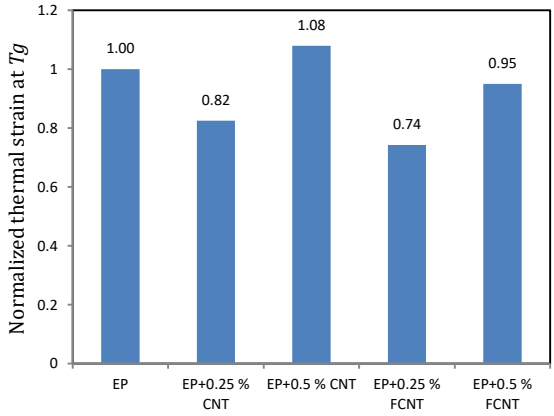

Figure 12. Normalized ε_{T_g} of the nanocomposites

3.2 SEM images

SEM images of the tensile test specimens' fracture surfaces were taken to show the dispersion quality of the CNTs into the epoxy resin. The images are shown in figures 13–16. As can be seen in Fig. 13, when there is 0.25 wt. % of MWCNTs into the epoxy matrix, MWCNTs are dispersed well into the matrix material. Furthermore, Fig. 14 illustrates that, when the wt. % of MWCNTs increased to 0.5 wt. %, the agglomeration of MWCNTs occurred in some regions; this resulted in reduced mechanical properties. Fig. 15 displays the homogenous dispersion of AFMWCNTs (0.25 wt. %) into the epoxy resin. Based on the figure, CNTs were uniformly distributed all over the matrix materials, which led to enhanced mechanical properties and decreased CTE. Moreover, as can be observed in Fig. 16, when AFMWCNTs with a 0.5 wt. % were added into the epoxy resin, accumulation of CNTs appeared in some regions.

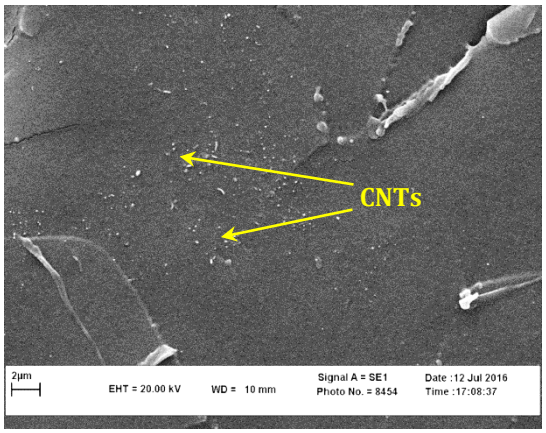

Figure 13. SEM images of the fracture surface of EP+0.25%CNTs

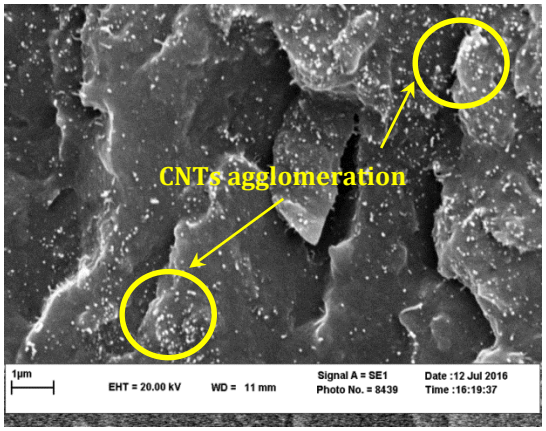

Figure 14 SEM images of the fracture surface of EP+0. 5%CNTs

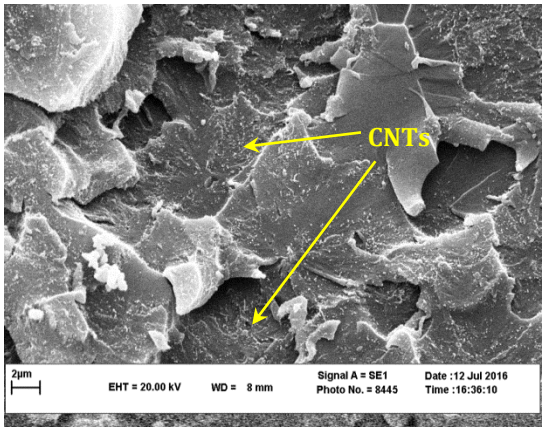

Figure 15. SEM images of the fracture surface of EP+0.25%AFCNTs

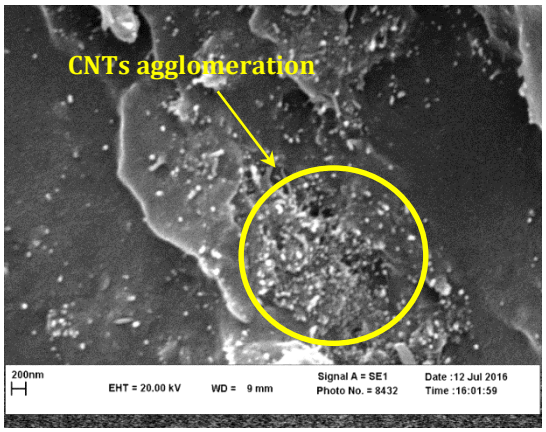

Figure 16. SEM images of the fracture surface of EP+0.5%AFCNTs

4. Conclusion

In this study, tensile and dilatometry test specimens of MWCNT/epoxy and AFMWCNT/epoxy nanocomposites were fabricated. In addition, 0.25 wt. % and 0.5 wt. % MWCNTs and AFMWCNTs were dispersed into an epoxy resin. Young's modulus, ultimate strength, strain at break, CTE, T_g, and thermal strain at T_g of the specimens were measured. The results indicated that amine functionalization of MWCNTs develops better dispersion of CNTs into the matrix material, which leads to the enhanced Young's modulus of the nanocomposite. The highest Young's modulus and the lowest CTE were related to the epoxy containing 0.25 wt. % AFMWCNTs. Furthermore, SEM images of the fracture surfaces and the tensile test results showed that, for both MWCNTs and AFMWCNTs, when the wt. % of CNTs increased to 0.5 wt. %, the CNTs tended to agglomerate into the epoxy matrix, which decreased the mechanical properties of the nanocomposite.

Acknowledgements

The authors would like to thank the Department of Material Science and Engineering at the Ferdowsi University of Mashhad for providing the tensile and dilatometer test units. This work was supported by a Ferdowsi University of Mashhad research grant (No. 3/38309).

Nomenclature

E	Young's modulus
S_{ut}	Ultimate strength
ε_b	Strains at break
T_g	Glass transition temperature
α	Coefficients of thermal expansion
L_0	Initial length of the specimen
ΔL	Sample length change
ΔL_{T_g}	Length increase of the specimen at T_g
ΔT	Temperature increase
ε_{T_g}	Thermal strain at the glass transition temperature

References

[1] Iijima S. Helical microtubules of graphitic carbon. *nature* 1991; 354(6348): 56-8.

[2] Her S-C, Yeh S-W. Fabrication and characterization of the composites reinforced with multi-walled carbon nanotubes. *Journal of nanoscience and nanotechnology* 2012; 12(10): 8110-5.

[3] Bukowska A, Bukowski W, Hus K, Depciuch J, Parlińska-Wojtan M. Synthesis and characterization of new functionalized polymer-Fe 3 O 4 nanocomposite particles. *Express Polymer Letters* 2017; 11(1).

[4] Ma P-C, Mo S-Y, Tang B-Z, Kim J-K. Dispersion, interfacial interaction and re-agglomeration of functionalized carbon nanotubes in epoxy composites. *Carbon* 2010; 48(6): 1824-34.

[5] Gojny F, Wichmann M, Köpke U, Fiedler B, Schulte K. Carbon nanotube-reinforced epoxy-composites: enhanced stiffness and fracture toughness at low nanotube content. *Composites Science and Technology* 2004; 64(15): 2363-71.

[6] Bal S, Borah J, Borgohain C. (2013). Microscopic Analysis of Mechanical Properties of Aligned Carbon Nanotube/Epoxy Composite. In *Advanced Nanomaterials and Nanotechnology* (pp. 347-65): Springer.

[7] Sharma K, Shukla M. Three-phase carbon fiber amine functionalized carbon nanotubes epoxy composite: processing, characterisation, and multiscale modeling. *Journal of Nanomaterials* 2014; 2014: 2.
[8] Kazemi H, Zandi K, Momenian H. Sonochemical Synthesis of Ca (OH) 2 Nanoparticles and Its Application in Preparation of MWCNT-Paraloid Nanocomposite. *Journal of Nanostructures* 2015; 5(1): 25-32.
[9] Ghorbanali M, Mohammadi A, Jalajerdi R. Synthesis Magnesium Hydroxide Nanoparticles and Cellulose Acetate-Mg (OH) 2-MWCNT Nanocomposite. *Journal of Nanostructures* 2015; 5(2): 175-81.
[10] Moaseri E, Maghrebi M, Baniadam M. Improvements in mechanical properties of carbon fiber-reinforced epoxy composites: a microwave-assisted approach in functionalization of carbon fiber via diamines. *Materials & Design* 2014; 55: 644-52.
[11] Shariati M, Farzi G, Dadrasi A. Mechanical properties and energy absorption capability of thin-walled square columns of silica/epoxy nanocomposite. *Construction and Building Materials* 2015; 78(0): 362-8.
[12] Shahrajabian H, Ahmadi-Brooghani SY, Ahmadi SJ. Characterization of Mechanical and Thermal Properties of Vinyl-ester/TiO2 Nanocomposites Exposured to Electron Beam. *Journal of Inorganic and Organometallic Polymers and Materials* 2013; 23(6): 1282-8.
[13] Parvaneh V, Shariati M. Experimental analysis of the low cycle fatigue of a spray-coated layered multi-walled carbon nanotubes/polyvinyl chloride nanocomposite. *Journal of Composite Materials* 2016; 50(11): 1555-62.
[14] Mehdizadeh P, Jahangiri H. Effect of carbon black content on the microwave absorbing properties of CB/epoxy composites. *Journal of Nanostructures* 2016; 6(2): 140-8.
[15] Hejri Z, Ahmadpour A, Seifkordi A, Zebarjad SM. Role of nano-sized TiO2 on mechanical and thermal behavior of starch/Poly (vinyl alcohol) blend films. *International Journal of Nanoscience and Nanotechnology* 2012; 8(4): 215-26.
[16] Lu Y-L, Ma J, Xu T-Y, Wang W-C, Jiang Y, Zhang L-Q. Preparation and properties of natural rubber reinforced with polydopamine-coating modified carbon nanotubes. *Express Polymer Letters* 2017; 11(1).
[17] Odegard GM, Gates TS, Nicholson LM, Wise KE. Equivalent-continuum modeling of nano-structured materials. *Composites Science and Technology* 2002; 62(14): 1869-80.
[18] Seidel GD, Lagoudas DC. Micromechanical analysis of the effective elastic properties of carbon nanotube reinforced composites. *Mechanics of Materials* 2006; 38(8–10): 884-907.
[19] Han Y, Elliott J. Molecular dynamics simulations of the elastic properties of polymer/carbon nanotube composites. *Computational Materials Science* 2007; 39(2): 315-23.
[20] Arash B, Wang Q, Varadan V. Mechanical properties of carbon nanotube/polymer composites. *Scientific reports* 2014; 4.
[21] Le M-T, Huang S-C. Modeling and Estimating the Effective Elastic Properties of Carbon Nanotube Reinforced Composites by Finite Element Method. *工程科技與教育學刊* 2014; 11(2): 145-58.
[22] Rostamiyan Y, Fereidoon A, Rezaeiashtiyani M, Mashhadzadeh AH, Salmankhani A. Experimental and optimizing flexural strength of epoxy-based nanocomposite: Effect of using nano silica and nano clay by using response surface design methodology. *Materials & Design* 2015; 69: 96-104.
[23] Rostamiyan Y, Fereidoon A, Rezaeiashtiyani M, Mashhadzadeh AH, Salmankhani A. Experimental and optimizing flexural strength of epoxy-based nanocomposite: Effect of using nano silica and nano clay by using response surface design methodology. *Materials & Design* 2015: 69, 96-104.